Journal of Superconductivity and Novel Magnetism
https://doi.org/10.1007/s10948-018-4749-x

ORIGINAL PAPER

Single- and Double-Layer Microwave Absorbers of Cobalt Ferrite and Graphite Composite at Gigahertz Frequency

Ismayadi Ismail[1] · Khamirul Amin Matori[1,2] · Zulkifly Abbas[2] · Muhamad Misbah Muhamad Zulkimi[1] · Fadzidah Mohd Idris[1] · Mohd Hafiz Mohd Zaid[2] · Nurfaziera Rahim[2] · Intan Helina Hasan[1] · Woon Hai Song[3]

Received: 7 February 2018 / Accepted: 22 May 2018

Abstract

Microwave absorbers of cobalt ferrite and graphite composite have been fabricated to investigate the broadening of absorption frequency by mixing small and large particles and comparing single- and double-layer composites in order to broaden the absorption frequency and to enhance multireflection and scattering of electromagnetic wave. CoO and Fe_2O_3 precursors were mechanically alloyed and sintered at 800, 900, 1000 and 1100 °C in order to synthesise various particle sizes and shapes. A mixed sample of powders sintered at the above mentioned temperatures was also formed. The morphological, phase, and magnetic properties of these samples were studied. Two series of samples have been synthesised which were single- and double-layer composites. Single-layer composite consisted of mixed particles, and their thickness parameters were varied. Double-layer composite was also prepared with various particle sizes of $CoFe_2O_4$ as a layer and graphene as another layer. The effect of these layers as matching and absorbing layer was studied. The degree of crystallinity of $CoFe_2O_4$ was increased with increase of sintering temperature. Microstructural study showed the evolution of particle size and shape subjected to sintering temperature. Arrhenius plot showed two stages of growth process with activation energy calculated at 26.85 and 83.091 kJ/mol. The critical size of single domain of this sample plotted from the coercivity against particle size was 63.44 nm. Single-layer composite with mixed particle size was not able to show good electromagnetic (EM)-wave absorption; however double-layer composite showed good return loss. The mechanism of the EM-wave absorption of double-layer composite was discussed in this paper.

Keywords Cobalt ferrite · Single layer · Double-layer structure · Microwave absorber · Reflection loss (RL)

1 Introduction

Recently, the demand for various kinds of microwave absorbers has increased in the frequency range of 1–20 GHz because of their twofold use, electromagnetic interference (EMI) shielding, and counter measure to radar detection [1]. Among the materials that have been used in such application such as ferrous alloy, a metallic material, ferrite exhibits an interesting behaviour, absorbing energy from electromagnetic wave, and presents the best relation between the absorber performance and its final thickness [2].

Ferrites have been used as an absorbing material in various forms, e.g. sheets, paints, films, ceramic tiles and powders, loaded in matrix composites or mixed with conducting materials [3, 4]. However, microwave absorber which only uses ferrites is not able to achieve wideband absorption. As an alternative method to achieve it, researchers have carried out research on double- or multilayer structure microwave absorber by combining magnetic characteristic materials (ferrite) and dielectric characteristic materials such as carbon black, carbon nanotubes (CNTs) and graphene [5–12]. The challenge in synthesising the microwave-absorbing materials is to produce ideal materials able to cover electromagnetic (EM) absorption over a wideband of frequency. Experimental data however have shown that by having a high reflection loss (RL) material, the frequency range is normally narrow [6–12]. Wideband

✉ Ismayadi Ismail
kayzen@gmail.com

[1] Institute of Advanced Technology, Universiti Putra Malaysia, 43400 Serdang, Selangor, Malaysia

[2] Physics Department, Faculty of Science, Universiti Putra Malaysia, 43400 Serdang, Selangor, Malaysia

[3] College of Engineering, Universiti Tenaga Nasional (UNITEN), Kampus Putrajaya, Jalan Ikram-UNITEN, 43000 Kajang, Selangor, Malaysia

Published online: 27 June 2018

absorbing materials however show low RL and less favourable in applications. Dosoudil et al. [13] have studied the influences of particle size of MnZn/NiZn ferrite filler hybrid composites with polyvynilchloride (PVC) matrix on the frequency dispersion of their complex permeability and microwave absorption performances. Interestingly, they reported that as the particle of the ferrite filler decreases, the matching frequency increases, matching thickness decreases, the bandwidth raises and the minimum return loss decreases. Small particles have shorter domain wall length than large particles, resulting in reducing the width of domain wall vibration and increasing vibration frequency. Small particles cause the increase of demagnetisation effect induced by domain wall motion and according to the equation reported in ref. [13]:

$$f_{\text{res}} = \frac{\mu_{\text{o}}\gamma\,(H_{\text{A}} + H_{\text{D}})}{2\pi} \tag{1}$$

where f_{res} is the resonance frequency, μ_{o} is $4\pi \times 10^{-7} H/\text{m}$ (the permeability of free space), γ is the gyromagnetic ratio, H_{A} is the magnetocrystalline anisotropy field and H_{D} is the demagnetisation field. The equation shows shat f_{res} is directly proportional to H_{D} caused by the small particles.

The objective of this paper is to synthesise and study the microwave-absorbing properties of single- and double-layer structures combining cobalt ferrites ($CoFe_2O_4$) and dielectric materials (graphite) in order to achieve a wideband absorption, and their microwave absorber properties will be evaluated. The active materials will be synthesised using sintered powders at different temperatures to obtain a mixture of small and big particles and various shapes in a composite. Different sizes of particles due to sintering resulted in various shapes and affects the shape anisotropy which subsequently influenced the frequency of resonance; hence, by mixing various sizes of particles and shapes in a composite, we would expect broad band frequency of EM wave absorption. Theoretically, a double-layer absorber is expected to exhibit better microwave absorption performance than a single layer because the matching layer allows most of the incident EM waves to easily enter into the absorber. Secondly, the interface between the matching layer and the absorbing layer can enhance the chance of multireflection and scattering, which is in favour of EM wave attenuation [14].

2 Methodology

2.1 Preparation of $CoFe_2O_4$

The starting materials for preparation of $CoFe_2O_4$ were cobalt oxide (CoO) and iron oxide (Fe_2O_3) with both having 99.5% of purity from Alfa Aesar. The starting powders were weighed according to targeted proportions and mixed using ball milling for homogeneity. The powder mixture was further milled using a SPEX8000D mill in a hardened steel vial together with ten grinding balls having a diameter of 12 mm each to get nanometer sized particles. The milling time and ball to powder weight ratio (BPR) were 6 h and 10:1, respectively, and were used to obtain nanoparticles as the starting powder. It was then sintered at 800, 900, 1000 and 1100 °C for 10 h using a heating rate of 4 °C/min. The morphology of the particles was studied with field emission scanning electron microscope (FESEM). Magnetic behaviour (hysteresis) of the ferrite samples were studied using vibrating sample magnetometer (VSM) at room temperature. The sintered powders were mixed together with a ratio of 1:1 to obtain distribution of particle sizes and shapes.

2.2 Preparation of Composite Microwave-Absorbing Material

Single-layer composite specimens for measurement of the microwave absorber properties were prepared by mixing sintered $CoFe_2O_4$ and epoxy resin with concentration of 60:40 by weight. The mixed liquid was then poured into the sample holder and dried at room temperature for 24 h. The composite was prepared with 2 mm thickness. Meanwhile, double-layer samples were also prepared with top layer composed of mixed particle size of cobalt ferrites, in a concentration of 60% (w/w) in epoxy matrix with method as mentioned earlier and the thickness maintained at 1 mm. Then, graphite/epoxy was poured on top of the bottom layer, in a concentration of 5% (w/w). The most important condition to develop single- and double-layer electromagnetic wave-absorbing materials is to maintain homogeneity and uniform distribution of filler particles. The main advantage of using epoxy is due to room temperature curing which helps to avoid voids and surface crack. The measurement of microwave-absorbing nanocomposites was carried out with vector network analyser (VNA) in X-band (8–12 GHz) and Ku-band (12–18 GHz) frequency range.

3 Results and Discussion

3.1 Phase Analysis of $CoFe_2O_4$

Figure 1 shows the XRD pattern of $CoFe_2O_4$ samples sintered at 800–1100 °C with increment of 100 °C. The overall pattern clearly indicates that the sintered samples are exclusively of cubic spinel structure. All seven peaks of the cobalt ferrite phase were evident in the sample at 800 °C, indicating a crystalline phase formation. The degree of crystallisation, as suggested by intensity counts

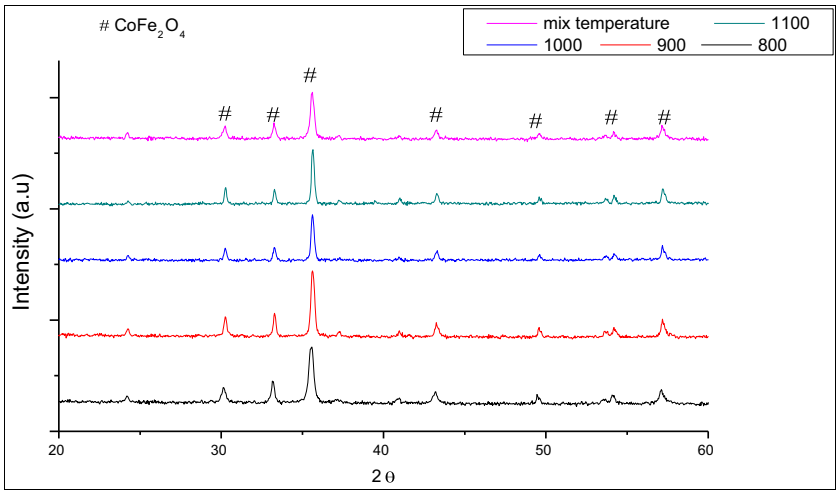

Fig. 1 XRD spectra of the $CoFe_2O_4$ at various sintering temperatures and mixed powder

in the sample was seen to increase strongly up to 1100 °C (Table 1). The intensity peaks increased with increasing sintering temperature, suggesting the increase of grain particle size and crystallinity of the materials. The peaks show cubic spinel structure with no extra lines, which indicates that samples form a single-phase polycrystal.

3.2 Microstructural Analysis

The morphology of sintered ferrite particle was examined by FeSEM and shown in Fig. 2. It was observed that the particle appeared to be spherical in nature with an average particle size increased with increasing sintering temperature. Meanwhile, Fig. 3 shows the histogram of particle size distribution for all samples sintered at 800, 900, 1000 and 1100 °C. Particle size of sample sintered at 800 °C was 58 nm, and sample sintered at 900 °C was around 63 nm. The average particle size of both samples sintered at 1000 and 1100 are 94 and 221 nm, respectively. The increase of average grain size shows the microstructural evolution of the samples. The microstructural evolution of these sintered samples can be described by adapting the sintering mechanism explained by ref. [15] which involved five stages in the process:

1) First initial stage is where no grain growth and mass transport of the sintered samples are by grain boundary diffusion.
2) Second initial stage occurs afterwards where no grain growth occurs and the mass transport of the sintered body is by lattice diffusion.
3) First intermediate and final stages later take place where lattice diffusion occurs without any grain growth of the samples.
4) Second intermediate and final stages where there is grain growth happening and lattice diffusion still playing the role.
5) Final intermediate stage where grain boundary diffusion occurs with no grain growth.

Figure 2a shows the appearance of necking process when sintered at 800 °C, indicating the growth development of the grains. Looking at Fig. 3a, b of samples sintered at 800 and 900 °C, the grain size distribution of 900 °C was broader

Table 1 XRD peak intensity and magnetic parameters of sintered and mixed samples

Temperature (°C)	Magnetisation (M_s) (emu/g)	Retentivity (M_r) (emu/g)	Coercivity (H_c) (G)	XRD peak intensity (counts)
800	56.26	29.79	1486.20	6571.80
900	30.27	15.96	1810.70	6722.85
1000	67.89	32.61	1407.80	6815.35
1100	88.63	33.21	860.40	6923.22
Mixed particles with different temperature	51.21	25.00	1561.50	6835.65

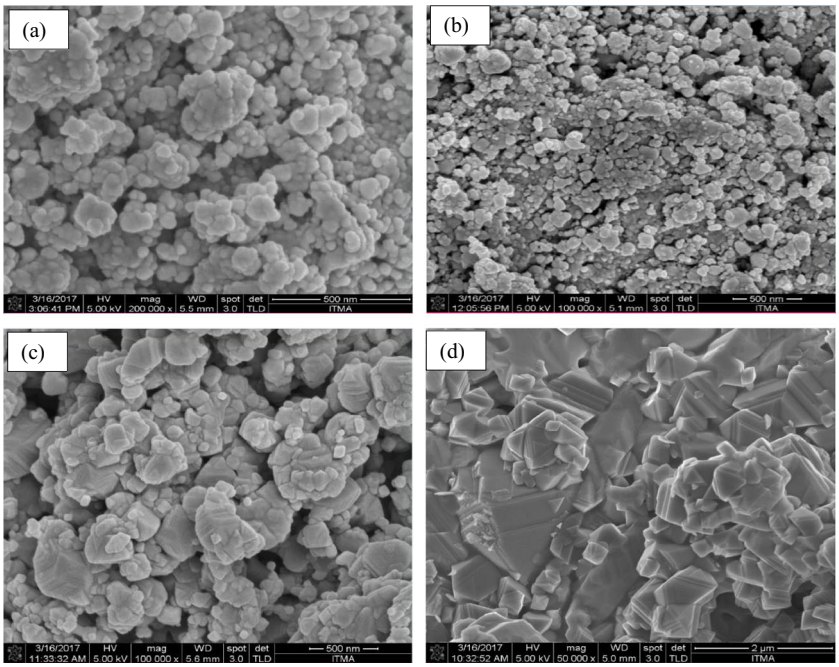

Fig. 2 FESEM microstructure of $CoFe_2O_4$ after being sintered at **a** 800, **b** 900, **c** 1000 and **d** 1100 °C for 10 h

compared with 800 °C, showing that a variable size of grains mixed and larger grain size is favourable for the development of domain walls. After the sintering temperature was increased to 1000 and 1100 °C, the grain size distribution moves to the right indicating the development of bigger grains where crystalline volume of the grains were

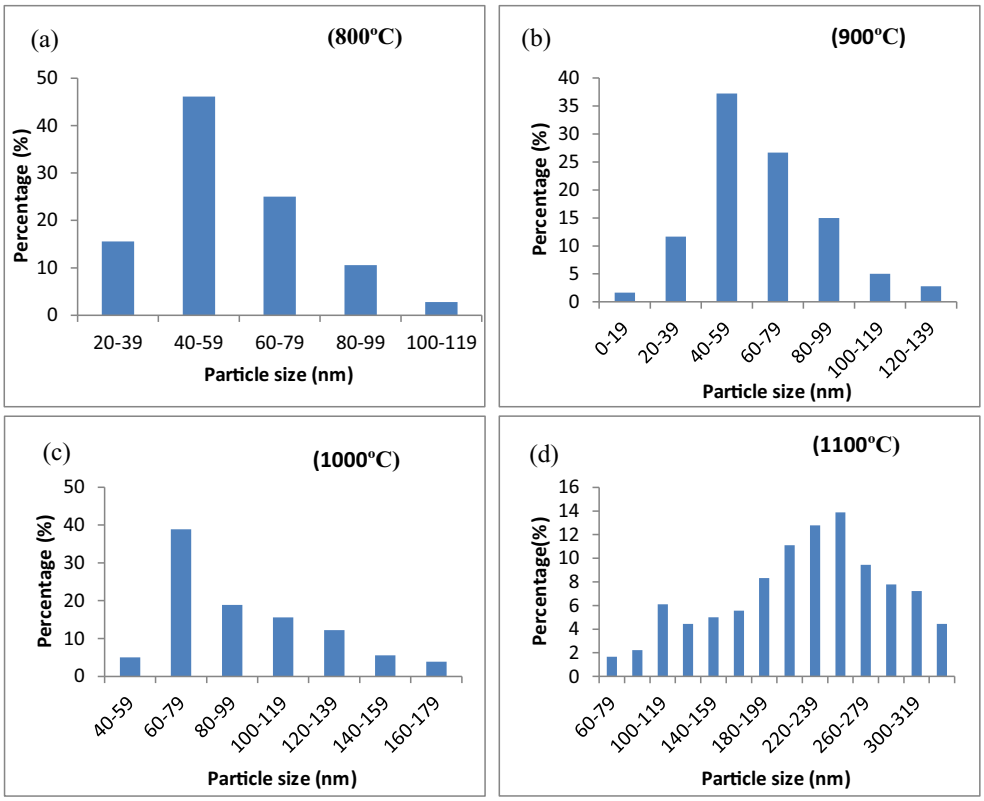

Fig. 3 Histogram of $CoFe_2O_4$ after being sintered at **a** 800, **b** 900, **c** 1000 and **d** 1100 °C for 10 h

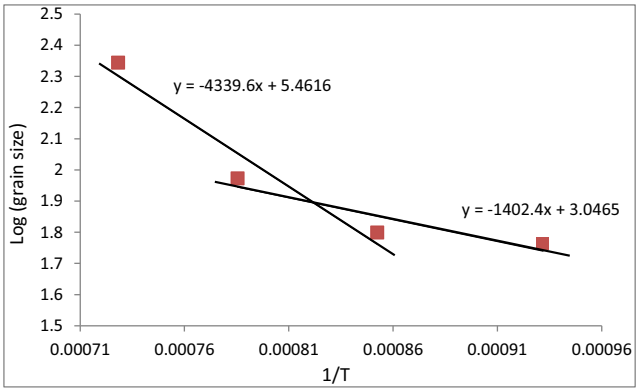

Fig. 4 Plot log D versus the reciprocal of absolute temperature (1/T (Kelvin))

increasing and in agreement with XRD results in Fig. 1. The increase in the number of bigger grains also contributed to the increase of magnetisation due to better crystallisation affecting the ordered magnetic spin.

One of the factors influencing the ferromagnetic resonance is domain wall susceptibility, X_w may be written as:

$$\chi_w = \frac{3\pi M_s D}{4\gamma} \tag{2}$$

where M_s is the saturation magnetisation, D is the average grain diameter and γ is the domain wall energy. From the formulae given, the domain wall motion is affected by the grain size and enhanced with the increase of grain size.

Coble's theory [16, 17] mentioned that from the behaviour of particle growth, the activation energy of grain growth can be predicted using the Arrhenius equation below:

$$d \ln k / \mathrm{d}T = Q/RT^2 \tag{3}$$

where k is the specific reaction rate constant, Q is the activation energy, T is the absolute temperature and R is the ideal gas constant. The value of k however can directly be related to grain size according to ref. [18], which results in the equation below:

$$\mathrm{Log}\ D = (-Q/2.303R)1/T + A \tag{4}$$

where T is the absolute temperature, A is the intercept and D is the grain size. By using (4), one can obtain a best-fitted straight-line plot of grain size including a plot of log D versus the $1/T$, as shown in Fig. 4. From (4), we obtained two slopes and correlated them to–Q/2.303R, and the value of the activation energy of grain growth (Q) can be calculated from the Arrhenius plot which were 26.851 and 83.091 kJ/mol. From these results, we speculated that the activation energy is related to the growth process of the microstructure which in turn influences the magnetic phase of the materials. Further study is needed to confirm this speculation.

3.3 Effect of Different Particle Sizes of $CoFe_2O_4$

Figure 5 shows that particles from sintering temperature of 800–1100 °C were mixed together having different sizes and shapes. Variation size of particle was thought to be possibly important for broad frequency-band absorption because the corresponding broad size and shape anisotropy fields would cause ferromagnetic resonances to occur over a wide range of frequencies. Basically, these phenomena could occur according to $\omega\tau = \gamma H_a$ where $\omega\tau =$ resonant angular frequency, $\gamma =$ gyromagnetic ratio, $H_a =$ total anisotropy field of a crystallite. The micrograph shows that $CoFe_2O_4$ particles were mixed with irregular, roundish, elongated shapes and well crystalline particles. The particle size of $CoFe_2O_4$ is between 20 and 140 nm with an average size of 78.26 nm. The small particles are agglomerated due to interactions of magnetic dipole between particles [19]. Smaller particles below a certain size contain a single domain, or few domains lead to a higher anisotropy field causing the magnetic moment harder to

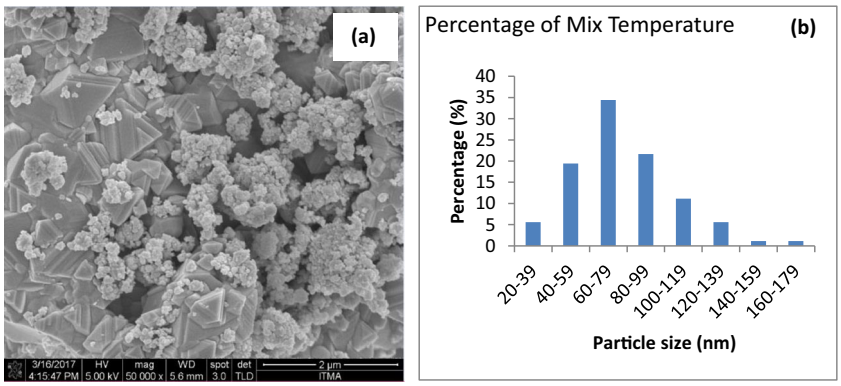

Fig. 5 **a** FeSEM micrograph of $CoFe_2O_4$ particles mixed with all sintered samples and **b** histogram of particle size distribution for the sample

reverse. By increasing the size-cum-shape of the particles (using sintering), accommodation of domain wall started to take place and easy displacement of magnetic spin resulted and affect the resonance frequency. Excellent absorption of EM wave in gigahertz range shown by nanomaterials is due to small size and shape anisotropy effects. Kodama [20], Zheng et al. [21] and Gazeau et al. [22] mentioned that surface spins of ferrite nanoparticles are disordered; the exchange coupling between the surface and core gives rise to a variety of spin distribution within a single-domain particle.

3.4 Magnetic Properties

The magnetic properties of sintered and mixed ferrites are shown in Fig. 6a, and the values of the saturation magnetisation, coercivity and retentivity are listed in Table 1. The hysteresis loop at room temperature explains the soft ferromagnetic nature of the sample. The M_S value decreases when sintered temperature is up to 900 °C and increasing for further sintering temperature. This decrease may be ascribed to the hard reversible displacement or domain wall movement in the direction of applied field. The harder the displacement, the smaller will be the value of M_S. The increase of saturation magnetisation with increase in sintering temperature is an indication that the average magnetic domain size of the particles is increasing and the atomic spins are getting more aligned with the direction of the applied field.

The coercivity values were found to increase as the sintering temperature increased from 800 to 900 °C, reaching a maximum value but decreasing from 900 to 1100 °C. This is due to the increase of the average particle size with sintering temperature. More domain walls were formed in larger particle size. Therefore, the contribution of wall movement to magnetisation or demagnetisation, which required lower energy than domain rotation, increases. Therefore, the larger grains are expected to have low coercivity [23]. The plot in Fig. 6b confirms the trend and gives a maximum coercivity value of 1407.80 G at 63.44 nm, respectively. Below critical size (red dotted line in Fig. 6b), the grain becomes a single domain, and within this size range, the coercivity reaches maximum because of the shape anisotropy and magnetocrystalline anisotropy.

3.5 Microwave-Absorbing Performance

3.5.1 The Influence of Physical Thickness and Double-Layer Structure on Reflection Loss

In order to investigate the electromagnetic wave absorption properties of the samples, the reflection loss (RL) was calculated

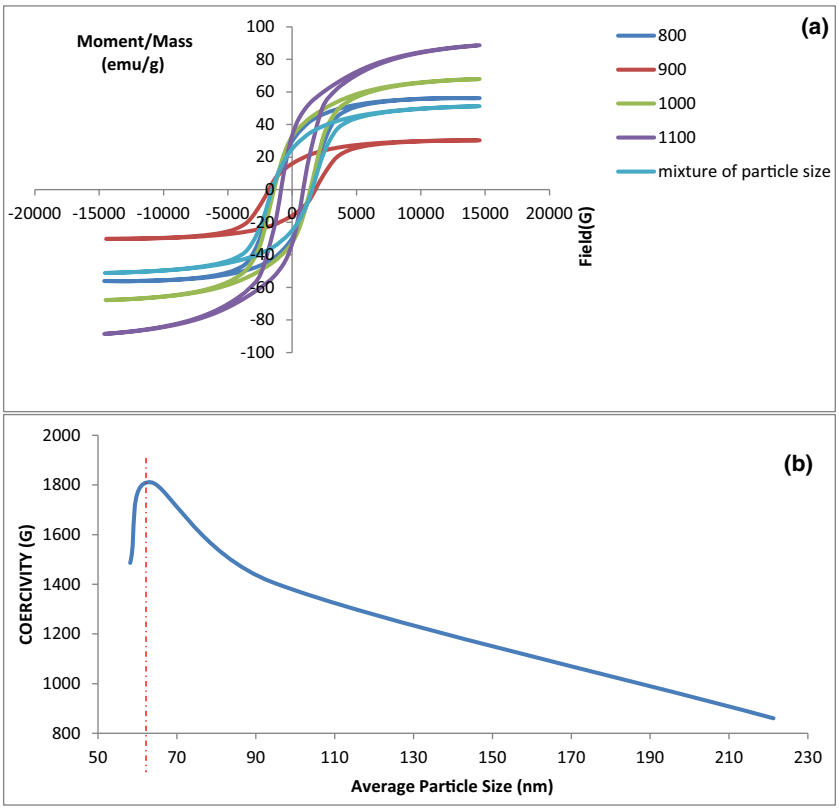

Fig. 6 **a** Hysteresis loops of all samples at room temperature and **b** coercivity versus average particle size for all sintered samples

and plotted in decibel (dB) by using the transmission line theory using the complex permittivity and permeability as follows:

$$\mathrm{RL} = 20\log\left|\frac{Z_{\mathrm{in}}-1}{Z_{\mathrm{in}}+1}\right| \tag{5}$$

where the normalised input impedance (Z_{in}) is given by the formula,

$$Z_{\mathrm{in}} = \sqrt{\frac{\mu_{\mathrm{r}}}{\varepsilon_{\mathrm{r}}}}\tanh\left(j\left(\frac{2\pi f d}{c}\right)\sqrt{\mu_{\mathrm{r}}\varepsilon_{\mathrm{r}}}\right) \tag{6}$$

where $\varepsilon_{\mathrm{r}} = \varepsilon' - j\varepsilon''$, $\mu_{\mathrm{r}} = \mu' - j\mu''$, f is the electromagnetic wave frequency (Hz), d is the thickness of the absorber (m) and c is the velocity of light in free space (m/s). Meanwhile the Z_{in} for double layer is given by the formula,

$$Z_{\mathrm{in}} = \frac{\sqrt{\frac{\mu_2}{\varepsilon_2}}\left(\sqrt{\frac{\mu_1}{\varepsilon_1}}\tanh\left(j\left(\frac{2\pi f d_1}{c}\right)\sqrt{\mu_1\varepsilon_1}\right)+\sqrt{\frac{\mu_2}{\varepsilon_2}}\tanh\left(j\left(\frac{2\pi f d_2}{c}\right)\sqrt{\mu_2\varepsilon_2}\right)\right)}{\sqrt{\frac{\mu_2}{\varepsilon_2}}+\sqrt{\frac{\mu_1}{\varepsilon_1}}\tanh\left(j\left(\frac{2\pi f d_1}{c}\right)\sqrt{\mu_1\varepsilon_1}\right)\tanh\left(j\left(\frac{2\pi f d_2}{c}\right)\sqrt{\mu_2\varepsilon_2}\right)} \tag{7}$$

where ε_1, ε_2, μ_1 and μ_2 are the complex permittivity and permeability of layers 1 and 2, respectively. d_1 and d_2 are thickness of layers 1 and 2, respectively, and f and c are similar to (6). Layer 1 is the absorption layer, and layer 2 is the matching layer as depicted by the double-layer structure model in Fig. 7. The RL of the electromagnetic wave of double-layer samples can be calculated by substituting (7) into (4) and the experimental results are represented in Fig. 8 and Table 2.

Figure 8a shows the result of reflection loss in decibels which corresponds to the S_{11} parameter for single-layer composite; the thicker the thickness, the lower the reflection of the sample, so the absorption will be higher. The $CoFe_2O_4$ has the highest value of reflection loss at 3 mm thickness which is -8 dB at a frequency of 12.5 GHz. It is good to clearly understand the meaning of the lower negative number of the reflection loss and vice versa. By having a lower negative number, it means a higher reflection of the sample, so, the absorption will be lower. By having a higher negative number, it means a lower reflection of the sample, so the absorption will be higher.

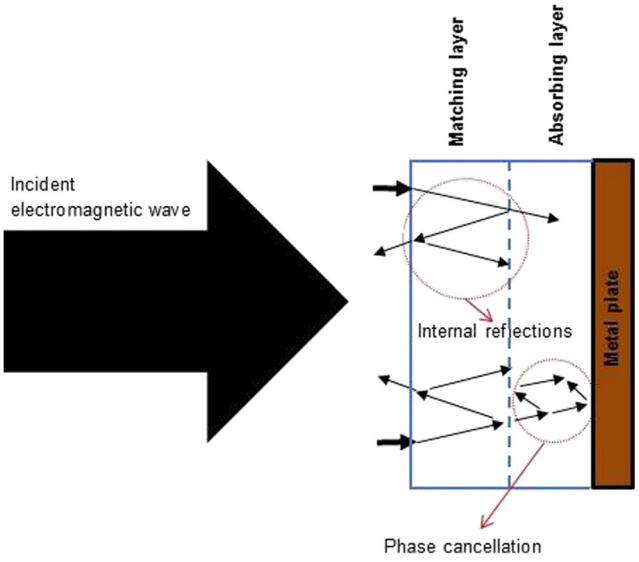

Fig. 7 Multiple internal reflections phenomenon of double-layering materials

Figure 8b shows results of multilayer structure with different thicknesses. G1_Co1 is nominated as graphene layer with 1 mm thick and cobalt ferrite with 1 mm thick where graphene is the matching layer and cobalt ferrite is the absorption layer. Meanwhile, G1_Co2 label is having a 3-mm total thickness with cobalt ferrite layer (absorbing layer) of 2 mm. Figure 8c shows the results of reflection loss of multilayer structure with an opposite layering structure from Fig. 8b. There are different results when the graphite was placed at the front and at the back during the test. The absorption of microwave can be improved by combining the proper electromagnetic impedance match [24]. The result shows a higher value of highest peak, and the frequency range was also broadened for both thicknesses (Table 2). The minimum reflection loss for 2 mm thickness is -11 dB within a frequency range below -10 dB at 0.7 GHz (Table 2) for cobalt ferrite placed in front (as matching layer) whereas when the cobalt ferrite was positioned at the back (as absorbing layer), the minimum reflection loss is -8.8 dB. For 3-mm thickness, the frequency range was not broad as the 2 mm multilayer samples when the cobalt ferrite was placed at the front (as matching layer), showing a minimum reflection loss of -15 dB, meanwhile when the cobalt ferrite was placed at the back (as an absorbing layer), the minimum reflection loss is -12.8 dB. It can be concluded that cobalt zinc ferrite layered for 2 mm with graphite have the best result for the multilayer part. The details of microwave-absorption properties of single and double layers are listed in Table 2.

Better electromagnetic wave absorption in the double-layer structure can be explained due to increment in the number of interfaces where there are multiple internal reflections at boundaries which results in phase cancellation.

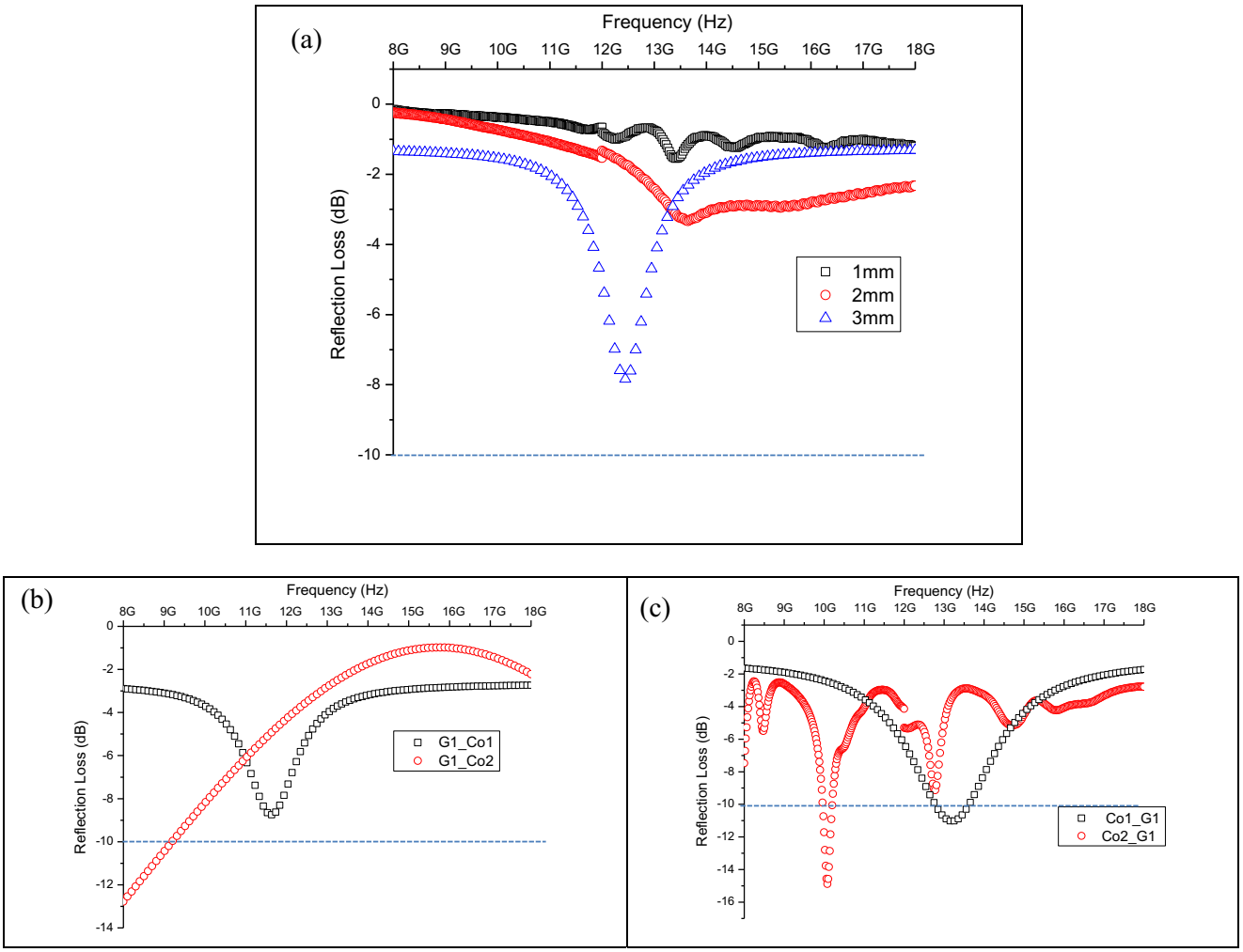

Fig. 8 Reflection loss of **a** single- and multilayer **b** graphite/cobalt ferrite and **c** cobalt ferrite/graphite with different thicknesses

Therefore, it will increase the overall absorption. Figure 7 shows the phenomenon of electromagnetic wave absorption in double-layer structure. For normal incidence of electromagnetic wave on double-layer structure of metal plate at first interface of matching layer, electromagnetic wave got partially reflected and partially transmitted into matching layer and became attenuated. It again gets re-reflected and re-transmitted by interface of absorbing and matching layer. After traveling into the absorbing layer of many internal reflections, multiple internal reflections and phase cancellation occurs during propagation. If material losses and these multiple internal reflections are included, the overall

Table 2 The details of single- and double-layer composites and their absorber properties

Composite	Thickness (mm)	Reflection loss (dB)	Frequency (GHz)	Bandwidth (≤ 10 dB)
Single-layer cobalt ferrite	1	− 1.0	13.4	–
	2	− 3.5	13.5	–
	3	− 8.0	12.5	–
Double-layer				
(i) Graphite/cobalt ferrite	2	− 8.8	11.7	–
	3	− 12.8	8.0	1.2
(ii) Cobalt ferrite/graphite	2	− 11	13.3	0.7
	3	− 15	10	0.5

absorption will increase because the maximum part of the electromagnetic wave is attenuates inside the layers [25–27]. It is interesting to note that these absorption results are obtained from the compositions which are not achieved as single-layer absorber.

4 Conclusion

The preparation and characterisation of $CoFe_2O_4$ and graphite for single layer and multilayer have been successfully carried out. The nanoparticle of sample can be obtained by milling for 6 h and sintered at a temperature range of 800–1100 °C. Even though various particle sizes of powders were mixed together, single-layer nanocomposites were not able to absorb good EM wave as expected. Multilayer nanocomposites on the other hand showed good return loss and variation of response resulted from playing around the matching and absorbing layer of the samples. The microwave-absorbing properties and the absorbing bandwidth of nanocomposites can be manipulated by adding the layer of the composites and the thickness of the sample

Funding Information This research is supported by Universiti Putra Malaysia (UPM), Malaysia, under Geran Putra Muda (GP-IPM/2017/9545400).

References

1. Abbas, S.M., Chandra, M., Verma, A., Chatterjee, R., Goel, T.C.: J. Compos.: Part A **37**, 2148 (2006)
2. Alexandre, R.B., Maria, L.G., Maria, C.S.: J. Magn. Magn. Mater. **320**, 864 (2008)
3. Hatakeyama, K., Inul, T.: IEEE Trans. Magn. **20**(5), 1261 (1984)
4. Suetake, K.: US Patent No. 3,623,099 (1971)
5. Khan, K.: J. Supercond. Nov. Magn. **27**, 453 (2013)
6. Durmus, Z., Durmus, A., Kavas, H.: J. Mater. Sci. **50**, 1201 (2015)
7. Das, S., Nayak, G.C., Sahu, S.K., Routray, P.C., Roy, A.K., Baskey, H.: J. Eng. **2014**, 1 (2014)
8. Vinayasree, S., Soloman, M.A., Sunny, V., Mohanan, P., Kurian, P., Anantharaman, M.R.: Compos. Sci. Technol. **82**, 69 (2013)
9. Shiri, N., Amirabadizadeh, A., Ghasemi, A.: J. Alloy Compd. **690**, 759e764 (2017)
10. Liang, K., Qiao, X.J., Sun, Z.G., Guo, X.D., Wei, L., Qu, Y.: J. Appl. Phys. A **123**, 445 (2017)
11. Ding, Y., Liao, Q., Liu, S., Guo, H., Sun, Y., Zhang, G., Zhang, Y.: Sci. Rep. **6**, 32381 (2016)
12. Vinayasree, S., Soloman, M.A., Sunny, V., Mohanan, P., Kurian, P., Joy, P.A., Anantharaman, M.R.: Jpn. J. Appl. Phys. **116**, 024902 (2014)
13. Dosoudil, R., Usakova, M., Franek, J., Slama, J., Gruskova, A.: IEEE Trans. Magn. **46**(2), 436 (2010)
14. Guo, S.L., Wang, L.D., Wang, Y.M., Wu, H.J., Shen, Z.Y.: Chin. Phys. B **22**(4), 044101 (2013)
15. Ismail, I., Hashim, M., Kanagesan, S., Ibrahim, I.R., Nazlan, R., Wan Ab Rahman, W.N., Abdullah, N.H., Mohd Idris, F., Bahmanrokh, G., Shafie, M.S.E.: J. Magn. Magn. Mater. **351**, 16 (2014)
16. Coble, R.L.: J. Appl. Phys. **32**, 787 (1961)
17. Shinde, T.J., Gadkari, A.B., Vasambekar, P.N.: Mater. Chem. Phys. **111**(1), 87 (2008)
18. Jarcho, M., Bolen, C.H., Thomas, M.B., Bobick, J., Kay, J.K., Doremus, R.H.: J. Mater. Sci. **11**, 2027 (1976)
19. Idris, F.M., Hashim, M., Ismayadi, I., Idza, I.R., Manap, M., Shafie, M.S.E.: IEEE Trans. Magn. **49**(11), 5475 (2013)
20. Kodama, R.H.: J. Magn. Magn. Mater. **200**, 359 (1999)
21. Zheng, H., Yang, Y., Zhou, M., Li, F.: Hyperfine Interact. **189**, 131 (2009)
22. Gazeau, F., Dubois, E., Hennion, M., Perzynski, R., Yu, R.: Europhys. Lett. **40**, 575 (1997)
23. Waje, S.B., Hashim, M., Yusoff, W.D.W., Abbas, Z.: Appl. Surf. Sci. **256**(10), 3122 (2010)
24. Jahanbin, T., Hashim, M.: J. Magn. Magn. Mater. **322**(18), 2684 (2010)
25. Folgueras, L.C., Rezende, M.C.: J. Mater. Res. **11**, 245 (2008)
26. Panwar, R., Agarwala, V., Singh, D.: AIP Conf. Proc. **1620**, 406 (2014)
27. Panwar, R., Puthucheri, S., Agarwala, V., Singh, D.: J. Electromagn. Waves Appl. **29**, 1238 (2015)